

Fluorescent carbazole dendrimers for the detection of nitroaliphatic taggants and accelerants

Andrew J. Clulow, Paul L. Burn,* Paul Meredith* and Paul E. Shaw

Received 3rd April 2012, Accepted 16th May 2012

DOI: 10.1039/c2jm32072j

The detection of explosive taggant 2,3-dimethyl-2,3-dinitrobutane (DMNB) and accelerant nitromethane (NM) by oxidative quenching of dendrimer fluorescence is examined. Two fluorescent dendrimers incorporating a 3,6-disubstituted-9-*n*-hexylcarbazole-based core and first-generation biphenyl-based dendrons linked directly or with acetylene bridges are reported. The dendrimers display good photoluminescence (PL) quantum yields in both solution and thin films and appropriate excited state energies for oxidation by the nitroaliphatic analytes. The dendrimer natural excited state lifetimes in solution of 6.8 and 7.4 ns were found to be significantly longer than previously reported fluorescent conjugated polymers and dendrimers for sensing applications. Steady-state PL quenching measurements in solution revealed the highest quenching efficiencies for the detection of nitroaliphatics reported to date of $59 \pm 1 \text{ M}^{-1}$ for DMNB and $78 \pm 1 \text{ M}^{-1}$ for NM. Furthermore, PL lifetime quenching measurements confirmed that the dendrimers were quenched by a predominantly collisional quenching mechanism. As such, the unprecedented quenching efficiencies with nitroaliphatics in solution are due to the combination of the long excited state lifetimes of the dendrimers and efficient collisional quenching. The fluorescence of dendrimer thin films was also reversibly quenched by exposure to pulses of sub-saturation concentrations of analyte vapours. However, in the thin film case the sensitivity towards DMNB was found to be greater than NM, highlighting the disparity between solution and thin film fluorescence quenching measurements.

Introduction

The prevailing global security situation means that the detection of explosives is of paramount importance in domestic environments and in current and past conflict zones. Much attention has been given to the detection of nitroaromatic explosive residues such as 2,4,6-trinitrotoluene (TNT) and 2,4-dinitrotoluene (DNT) due to their common usage in explosive compositions and landmines.^{1–6} Plastic explosives based on organic nitramines and nitrate esters have also received considerable attention.^{7,8} In contrast, there have been relatively few reports on the efficient fluorescence quenching-based sensing of nitroaliphatics such as 2,3-dimethyl-2,3-dinitrobutane (DMNB) and nitromethane (NM).^{9–13} DMNB is a highly volatile tagging agent in commercially manufactured plastic explosives and hence is an important target analyte for detection.¹⁴ NM is highly volatile and while it is has low detonation sensitivity in its neat form, when mixed with a variety of chemicals such as acids, bases, fuels and inorganic oxidants, it yields explosive compositions. NM is therefore used in

explosives since it is safer to ship and store when compared with nascent high-explosives.¹⁵

Detection of explosive analytes by oxidative fluorescence quenching is effective for materials that have a high electron affinity such as nitroaromatics. As a generic technique, fluorescent quenching has the potential to deliver rapid and sensitive detection with simple, low cost instrumentation suitable for portable or in-field use. In the detection process, the fluorescence sensing material is optically excited. If the analyte of interest is in the environment under scrutiny and has a suitable electron affinity the sensor is quenched by oxidation of the exciton thus providing a signal change. While in principle DMNB and NM can be detected by this method, in practise the response from the fluorescent sensing element is often very weak,^{11,16} a fact that has severely hindered the development of suitable sensing fluorophores. Herein we exploit the primarily collisional nature of fluorescence quenching by DMNB and NM in solution by creating sensing materials with long natural radiative lifetimes and appropriate energy levels. These molecules enable the detection of DMNB and NM in solution at levels comparable to those of higher electron affinity analytes^{17,18} and with the best sensitivity for nitroaliphatics reported to date.^{6,13} The sensing capabilities of thin dendrimer films are then evaluated and comparisons drawn with the solution based quenching assay.

Centre for Organic Photonics & Electronics, The University of Queensland, Brisbane, Queensland, 4072, Australia. E-mail: p.burn2@uq.edu.au; meredith@physics.uq.edu.au

Results and discussion

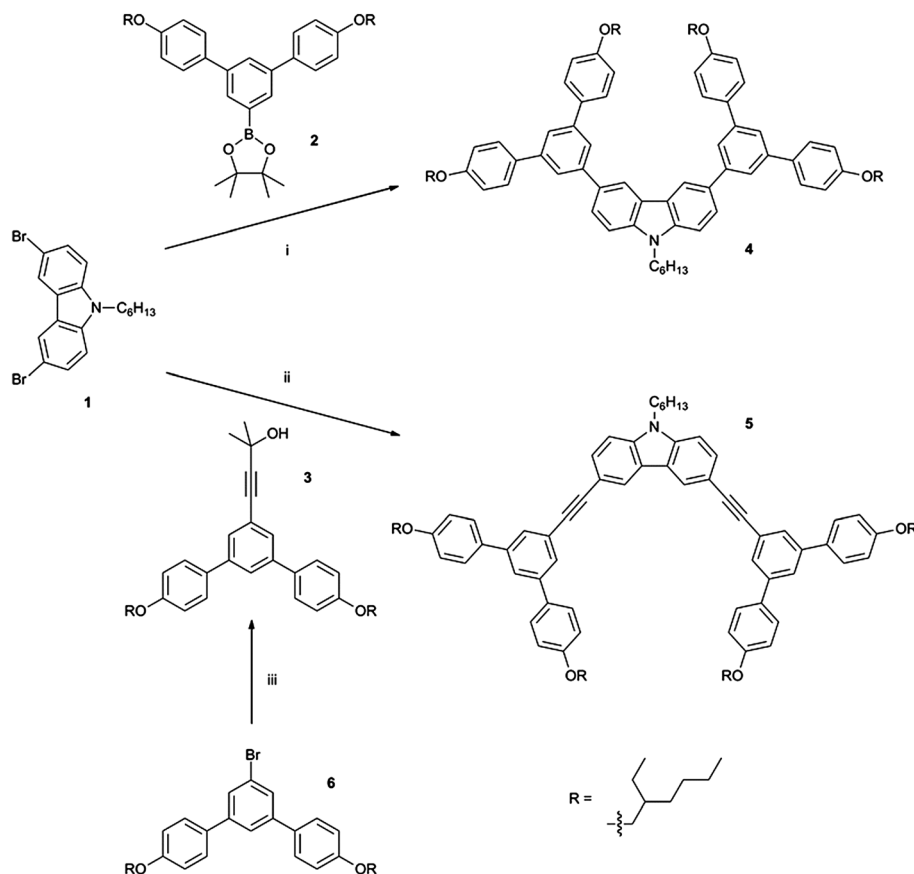
Dendrimer synthesis and physical properties

The structures and syntheses of the two dendrimers developed are shown in Scheme 1. The dendrimers are comprised of first generation biphenyl dendrons with 2-ethylhexyloxy surface groups and a carbazole-based core. Recent reports have suggested that materials containing carbazole units can display high affinities for DMNB in solution,^{6,13} however the origin of this affinity has not been explored. The dendrimers of this work were therefore designed to determine the influence of the carbazole unit on the sensitivity towards nitroaliphatic analytes and whether the affinity for the analytes in solution could be translated to the solid state. Dendrimer **4** has the dendrons directly attached to the carbazole unit while dendrimer **5** has the dendrons linked to the carbazole unit *via* acetylene moieties. As illustrated in Scheme 1 a convergent synthetic strategy was chosen in which functionalised dendrons **2** and **3** were prepared before attachment to the dibrominated carbazole **1**. The key step in the synthesis of each dendrimer was a metal-catalysed cross coupling. Dendrimer **4**, in which the dendrons are directly attached to the carbazole unit, was formed by a standard Suzuki reaction with the boronate ester focussed dendron **2**¹⁹ in a 52% yield. In the case of dendrimer **5** a biphasic Sonogashira coupling, in which the aqueous base deprotects acetylene **3** prior to coupling, gave the required material in a 47% yield. Dendron **3**

was itself formed by a Sonogashira reaction from the corresponding bromide focussed dendron **6**.¹⁹ Gel permeation chromatography showed that both dendrimers were mono-disperse and their hydrodynamic radii calculated from the \bar{M}_w s²⁰ were 8.4 Å and 9.1 Å for **4** and **5**, respectively. Differential scanning calorimetry gave glass transition temperatures of 37 °C for **4** and 25 °C for **5**.

Photophysical and electrochemical properties

For dendrimers **4** and **5** to be able to detect DMNB and NM by fluorescence quenching there are two minimum requirements: first, they must have detectable (preferably strong) fluorescence under excitation with UV or visible radiation; and second, their energetic structure must enable photoinduced electron transfer from the excited fluorophore to the ground state analyte (*i.e.*, oxidation of the dendrimer singlet exciton). The second requirement demands a negative energy difference between the excited state ionisation potential of the fluorophore and the ground state analyte electron affinity. This difference (and the general energetic landscape) was estimated *via* electrochemistry and optical spectroscopy by taking the energy difference between the calculated or measured reduction potentials of the analyte and the fluorescent dendrimers. The optical absorption and photoluminescence (PL) spectra of dendrimers **4** and **5** dissolved in dichloromethane are shown in Fig. 1. The onset of absorption



Scheme 1 Synthesis of dendrimers **4** and **5**. Conditions and reagents: (i) Pd(PPh₃)₄, PhMe, *tert*-BuOH, aq. K₂CO₃, 100 °C, N₂, 52%. (ii) Pd(PPh₃)₄, CuI, PhMe, aq. NaOH, *n*-Bu₄NBr, 80 °C, N₂, 47%. (iii) Pd(PPh₃)₄, CuI, 2-methylbut-3-yn-2-ol, piperidine, 80 °C, N₂, 91%.

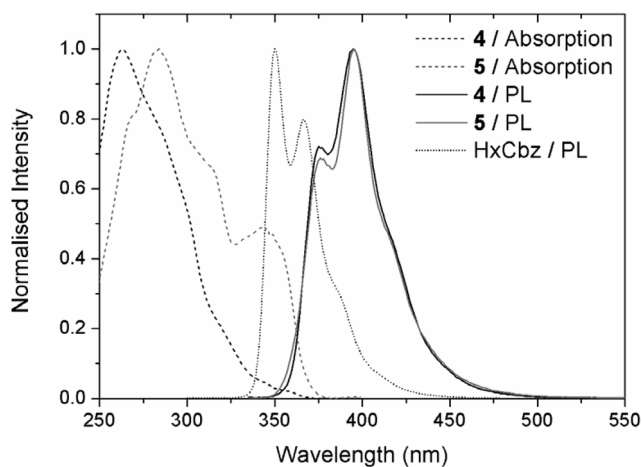


Fig. 1 Absorption and PL spectra of **4** and **5** in dichloromethane solution. The PL spectrum of unsubstituted 9-*n*-hexylcarbazole (HxCbz) is included for comparison.

for both dendrimers is around 375 nm although dendrimer **5** has much stronger absorption at the longer wavelengths due to the linking acetylene moieties. Both dendrimers have identical PL spectra with emission peaks at 375 nm and 395 nm and shoulders at 412 nm and 438 nm. The emission is red-shifted compared to the bare 9-*n*-hexylcarbazole core (Fig. 1) that displays emission peaks at 350 nm and 366 nm with shoulders at 384 nm and 405 nm. This observation is consistent with an extension of the conjugation of the emissive chromophore in **4** and **5** relative to the unsubstituted core. The photoluminescence excitation (PLE) spectra correlate well with the absorption of each dendrimer at detection wavelengths between 335 nm and 475 nm, suggesting that emission is from a single excited state of comparable energy for both **4** and **5**. No evidence of emission from the dendrons was observed showing that energy is transferred from the dendrons to the emissive chromophore. Solution photoluminescence quantum yields (PLQYs) were recorded in dichloromethane by the relative method using quinine sulfate as the standard²¹ and were found to be 0.19 ± 0.01 and 0.23 ± 0.01 for **4** and **5** respectively. The time-resolved PL decays at 400 nm in toluene solutions were measured to determine the natural excited state lifetime for each of the dendrimers. For dendrimer **4** the natural radiative lifetime was 7.4 ns and that of **5** was of similar magnitude at 6.8 ns. The combination of long fluorophore lifetime with lower PLQY implies a slow radiative decay rate for the active chromophore allowing a longer sampling time for quenching interactions.

The absorption and PL spectra of thin films of the dendrimers are shown in Fig. 2. The absorption spectra are similar to their solution counterparts with only slight red shifts in the peaks and shoulders observed. The thin film PL spectra of **4** and **5** are also comparable to that in solution except in the latter case there was a tail in the PL at the red end of the spectrum consistent with fluorophore aggregation in the solid state. This suggests that the first-generation biphenyl dendrons are sufficient to prevent significant aggregation of the carbazole chromophores when bound directly to the core. However, separation of the dendrons from the carbazole by addition of the bridging acetylene moieties results in a less sterically encumbered structure and greater

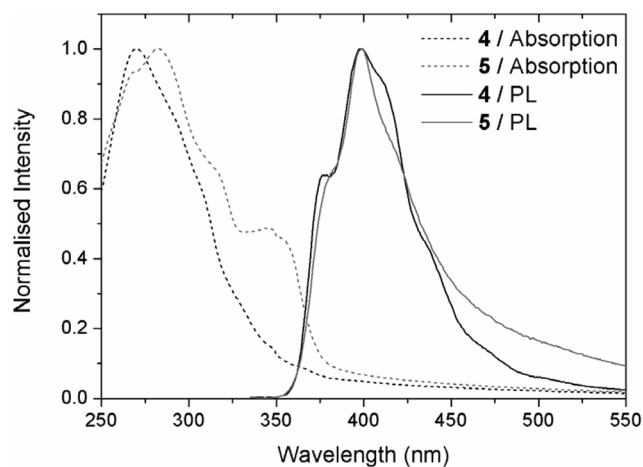


Fig. 2 Thin film absorption and PL spectra of dendrimers **4** and **5**.

aggregation. The PLQYs of the dendrimer thin films were found to be similar to their solution PLQYs being 0.27 ± 0.06 and 0.17 ± 0.02 for **4** and **5** respectively. The decrease in the PLQY of **5** in the solid state is consistent with the proposed fluorophore aggregation increasing non-radiative decay rates in the thin films. The increase in PLQY of biphenyl-substituted carbazoles such as **4** in thin films has been observed previously and is attributed to the restriction of intramolecular bond rotations eliminating non-radiative decay pathways in the solid state.²²

We used Cyclic (CV) and Differential Pulse (DPV) Voltammetry in combination with the optical energy gap to estimate the reduction potentials for **4** and **5**. CV showed that both the dendrimers underwent chemically reversible oxidations and for **5** DPV was used to determine the $E_{1/2}$. The $E_{1/2}$ s for **4** and **5** were 0.71 V and 0.75 V respectively versus the ferrocenium–ferrocene (Fc^+/Fc) couple. The $E_{1/2}$ s for the reductions lay outside the electrochemical window and so we estimated the reduction potentials by adding the energy of the optical gap. To calculate the optical gap we used a standard method: first, the absorption and PL spectra were rescaled by dividing the absorbance by photon energy (in eV) and PL by the photon energy cubed;²³ second, the spectra were normalised to the lowest energy absorption feature and the highest energy emission feature; and finally, the crossover point of the rescaled absorption and emission plots was taken as the optical energy gap. Using this method the optical gap was determined to be 3.4 eV for both dendrimers giving estimated reduction potentials of approximately -2.7 V for both **4** and **5** versus the Fc^+/Fc couple. The first reduction potential of DMNB has been reported as -2.2 V versus the Fc^+/Fc couple.⁹ The first reduction potential of NM has not been measured directly by cyclic voltammetry as it decomposes on electrode surfaces in a four-electron process liberating methylhydroxylamine.²⁴ However, based on the fact that DMNB and NM are simple nitroaliphatic molecules a similar first reduction potential would be expected. The difference of 0.5 V between the reduction potentials of the dendrimers and the analytes is greater than the reported exciton binding energies in organic semiconductors, which are often around 0.4 eV.²⁵ Therefore **4** and **5** both fulfil the two fundamental criteria for detection of nitroaliphatic analytes by oxidative fluorescence quenching.

Solution quenching measurements

The affinity (quenching efficiency) of an analyte for a particular fluorophore is generally quantified by steady-state Stern–Volmer measurements in solution. In such an experiment the quenching efficiency (loss of fluorophore emission) as a function of the analyte concentration is determined under steady-state illumination. Changes in absorption and fluorescence were monitored as known concentrations of analytes were added to a toluene solution of constant dendrimer concentration. Attenuation of the excitation beam and inner-filter effects caused by analyte absorption were corrected by our previously reported method.²⁶ The corrected data was then fitted to the Stern–Volmer equation for low quencher concentrations,¹⁷ given by

$$\begin{aligned} \frac{F_0}{F} &= 1 + \left\{ K_s + \frac{k_q}{k_r + k_{nr}} \right\} [Q] = 1 + \{ K_s + K_c \} [Q] \\ &= 1 + K_{sv} [Q] \end{aligned} \quad (1)$$

where F_0 is the integrated PL intensity in the absence of the analyte, F is the integrated PL intensity after analyte addition, K_s is the quenching efficiency due to the static binding of quencher molecules, K_c is the quenching efficiency due to collisional interactions with quencher molecules, k_q is the bimolecular quenching rate constant, k_r is the radiative decay rate constant, k_{nr} is the non-radiative decay rate constant, $[Q]$ is the quencher concentration and K_{sv} is the Stern–Volmer quenching constant for the analyte. The Stern–Volmer quenching constant thus determined is a combination of static binding efficiency (K_s) and the branching ratio of the rate of bimolecular quenching to all other intramolecular decay processes occurring (K_c). The steady-state Stern–Volmer plots obtained for the dendrimers with the analytes NM and DMNB are shown in Fig. 3. All runs were repeated in triplicate with separate analyte solutions and the data from each run combined to give the overall Stern–Volmer plots. Linear plots were obtained for both analytes with intercepts close to the theoretical value of 1.0.

The Stern–Volmer results are summarised in Table 1 and we believe that the quenching constants observed with the nitroaliphatic reagents NM and DMNB are the largest reported to date. The Stern–Volmer analyses gave K_{sv} values of $78 \pm 1 \text{ M}^{-1}$ and $59 \pm 1 \text{ M}^{-1}$ for **4** and $67 \pm 1 \text{ M}^{-1}$ and $55 \pm 1 \text{ M}^{-1}$ for **5** with NM and DMNB respectively. The overall magnitude of quenching was observed to follow the trend $\text{NM} > \text{DMNB}$ for both dendrimers and it was found on average that the fluorescence of **4** was quenched more effectively than **5** by both of the analytes.

The steady-state Stern–Volmer measurement does not give any information as to whether the observed quenching is due to a static process (the analyte forms a ground state ‘dark complex’ with the fluorophore prior to photoexcitation) or a collisional process (the analyte interacts briefly with the fluorophore in its photoexcited state). Therefore to further probe the underlying mechanism, time-resolved fluorescence quenching measurements were performed. By equating the observed fluorescence lifetime with the reciprocal of the sum of all decay processes occurring, the lifetime Stern–Volmer equation can be written as²³

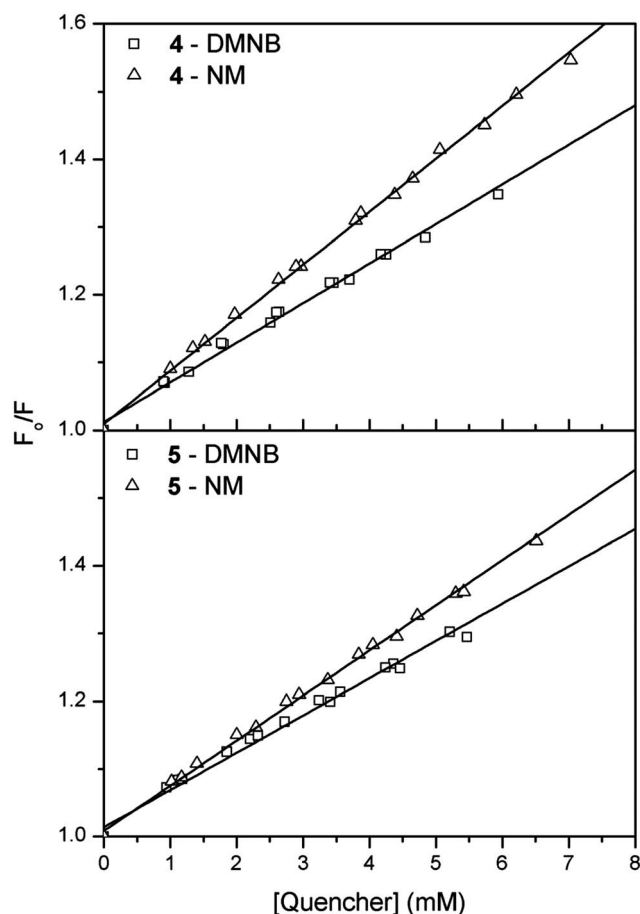


Fig. 3 Steady-state Stern–Volmer plots for **4** and **5** with NM and DMNB in toluene solution.

$$\begin{aligned} \frac{\tau_0}{\tau} &= \left\{ \frac{k_r + k_{nr} + k_q [Q]}{k_r + k_{nr}} \right\} = 1 + \left\{ \frac{k_q}{k_r + k_{nr}} \right\} [Q] \\ &= 1 + \tau_0 k_q [Q] = 1 + K_c [Q] \end{aligned} \quad (2)$$

where τ_0 is the radiative lifetime in the absence of quencher, τ is the radiative lifetime after analyte addition and K_c is the collisional portion of the Stern–Volmer constant as seen in eqn (1). The change in fluorescence lifetime observed upon the addition of analyte is due to collisional quenching by the analyte and hence the K_c provides a measure of the quenching caused by collisional interactions alone. The difference between the experimentally determined K_{sv} and K_c is due to static interactions (K_s) that quench the fluorescence by reducing the effective concentration of fluorophore but do not change the observed fluorescence lifetime.

Table 1 Summary of solution and thin film PL quantum yields (PLQYs), PL lifetime, steady-state Stern–Volmer constant (K_{sv}) and collisional quenching constant (K_c) data

Dendrimer/ analyte	Solution PLQY	Thin film PLQY	Solution lifetime (ns)	$K_{sv} (\text{M}^{-1})$	$K_c (\text{M}^{-1})$
4 /NM	0.19	0.27	7.4	78 ± 1	75 ± 1
4 /DMNB				59 ± 1	59 ± 1
5 /NM	0.23	0.17	6.8	67 ± 1	62 ± 1
5 /DMNB				55 ± 1	49 ± 1

The time-resolved Stern–Volmer measurements were performed using similar analyte concentrations as the steady-state measurements, and changes in the fluorescence lifetime were monitored at 400 nm with each analyte addition. In these experiments corrections for analyte absorption were not required as attenuation of the excitation beam only affects the PL intensity and not the PL decay rate. The normalised lifetime data were fitted with single exponential decays convoluted with the recorded instrument response function (IRF). The lifetime quenching data collected for **4** and **5** is displayed in Fig. 4 and this shows a clear decrease in the fluorescence lifetime upon addition of the analytes. The corresponding lifetime Stern–Volmer plots are displayed in Fig. 5.

The measured collisional Stern–Volmer constants, K_c , were essentially the same as the steady-state Stern–Volmer constants (Table 1) revealing that the fluorescence of the dendrimers is predominantly quenched in solution by a collisional mechanism. High levels of collisional quenching by nitroaliphatics have been observed previously and is attributed to their inability to engage in π – π interactions with the conjugated dendrimers.^{17,18} What is remarkable however, is the magnitude of the K_{sv} and K_c constants with **4** and **5**, which are much larger than those previously published. By way of example, an earlier reported dendrimer possessing the same first-generation biphenyl

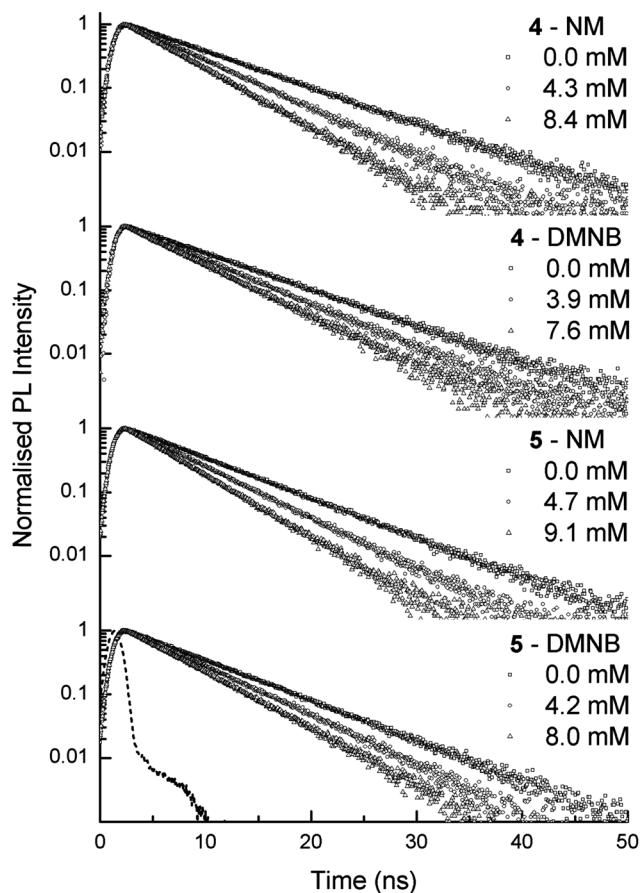


Fig. 4 Fluorescence lifetime quenching of **4** and **5** by NM and DMNB in toluene solution; dashed line indicates instrument response function (IRF).

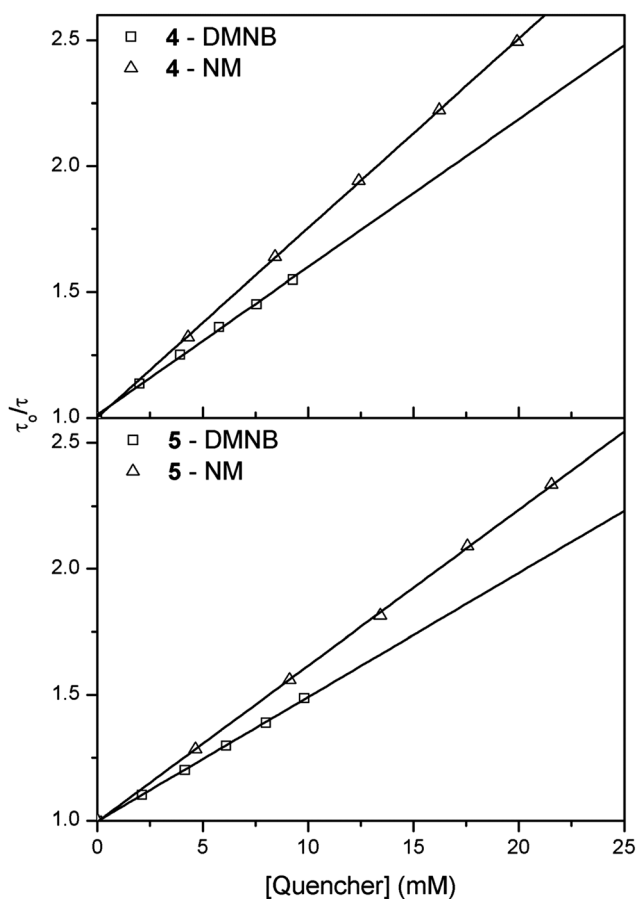


Fig. 5 Lifetime Stern–Volmer plots for dendrimers **4** and **5** with NM and DMNB in toluene solution.

dendrons and a bifluorene core¹⁸ had a steady-state K_{sv} of only $5 \pm 1 \text{ M}^{-1}$ for DMNB in spite of it having a higher PLQY and the interactions also being primarily collisional. Comparison of the performance of the dendrimers of this work with conjugated polymer systems is more difficult as the collisional Stern–Volmer constant determined by photoluminescence lifetime analysis possesses a contribution from delayed static quenching by diffusion of the exciton formed along the polymer chain.¹⁸ There is only a single report of the same lifetime Stern–Volmer analysis undertaken with DMNB and a conjugated polymer, poly(9,9-dioctylfluorene-2,7-diyl).¹⁸ In that work 30% of interactions of the polymer and analyte in solution were static, and the K_{sv} was also an order of magnitude lower ($5 \pm 1 \text{ M}^{-1}$)¹⁸ than the carbazole containing dendrimers of this current work. Indeed, in many cases static binding of analytes has been observed to be the dominant quenching mechanism for conjugated polymers.^{27,28}

We also determined the bimolecular collisional quenching rate constants (k_q) for each analyte using the observed natural lifetimes and collisional Stern–Volmer constants (eqn (2)). The bimolecular quenching rate constants were all found to be on the order of 10^9 – $10^{10} \text{ M}^{-1} \text{ s}^{-1}$. These values are in the range typical of diffusion-controlled rate constants²⁹ in solution indicating that quenching of the fluorophore by the analytes is highly efficient with most collisions resulting in quenching. Based on these results it would be reasonable to assign the observed trend in relative quenching efficiencies, NM > DMNB, to the smaller

molecular volume of NM that allows it to diffuse to a fluorophore more rapidly than DMNB. The key to the high quenching affinities with these new dendrimers is their relatively long singlet excited state lifetimes. While **4** and **5** have excited state lifetimes of 7.4 ns and 6.8 ns respectively, the previously reported first-generation dendrimers with bifluorene containing chromophores have lifetimes an order of magnitude shorter at 0.8 ns,¹⁸ and conjugated polymers typically have lifetimes of around a nanosecond.^{9,28} The observed dendrimer PL lifetimes of this work are about half those reported for unconjugated carbazole chromophores.³⁰ Hence, we have exploited the direct correlation between the natural fluorescence lifetime and the dominance of collisional quenching interactions to maximise the quenching response towards the nitroaliphatic analytes in solution. These results provide important insight for the design of more effective sensing materials: for analytes that display predominantly collisional quenching, such as nitroaliphatics, the highest quenching affinities are achieved by maximising the natural fluorescence lifetime of the sensing molecule.

Thin film quenching measurements

The fluorescence quenching effects that were observed in the solution-based measurements were translated into a detectable quenching response in the solid state. Thin films of dendrimers **4** and **5** of ~50 nm thickness were spin-cast onto fused silica substrates from toluene solutions and the PL of the films at 400 nm ($\lambda_{\text{exc}} = 320$ nm) was monitored over time. Natural photodegradation of the dendrimer films was observed with 35–50% of the initial fluorescence intensity lost within the first 30 minutes of continuous exposure to 320 nm radiation.

The films were exposed to a flow of nitrogen ($16.7 \text{ cm}^3 \text{ s}^{-1}$) throughout the measurements and this served as the carrier gas flow for the introduction of analyte vapours. With the nitrogen flow held constant by a mass flow controller the analytes were introduced by injecting known volumes of air presaturated with analyte into the carrier gas stream over 1 second. Such transient exposure measurements allow for a pulse of analyte of sub-saturation concentration to be introduced and the reversibility of the quenching interactions evaluated. The saturated vapour concentrations of DMNB and NM have been reported to be 2.7 ppm and 41300 ppm respectively.^{9,31}

Reversible fluorescence quenching responses were observed upon exposure of dendrimer **4** films to both DMNB and NM (Fig. 6). A 3% quenching response was detected on exposure to 1.5 ppm of DMNB vapour and the fluorescence recovered to the baseline within 20 seconds under the flow of nitrogen. Injection of smaller quantities of DMNB gave a corresponding decrease in the quenching response of the film with the response to 0.6 ppm DMNB being beyond the limit of reliable detection. Repeated injections of 2000 ppm of NM vapour into the carrier gas flow gave reversible quenching responses from 15–25% and quenching down to 500 ppm NM was observed. In all cases the baseline level of fluorescence was almost completely recovered within 10 seconds of NM exposure. In contrast to the results from the solution measurements the films display a greater quenching efficiency for DMNB in the solid state. The average initial quenching for DMNB was approximately $2\% \text{ ppm}^{-1}$ compared to around $0.01\% \text{ ppm}^{-1}$ for NM. The difference in signal

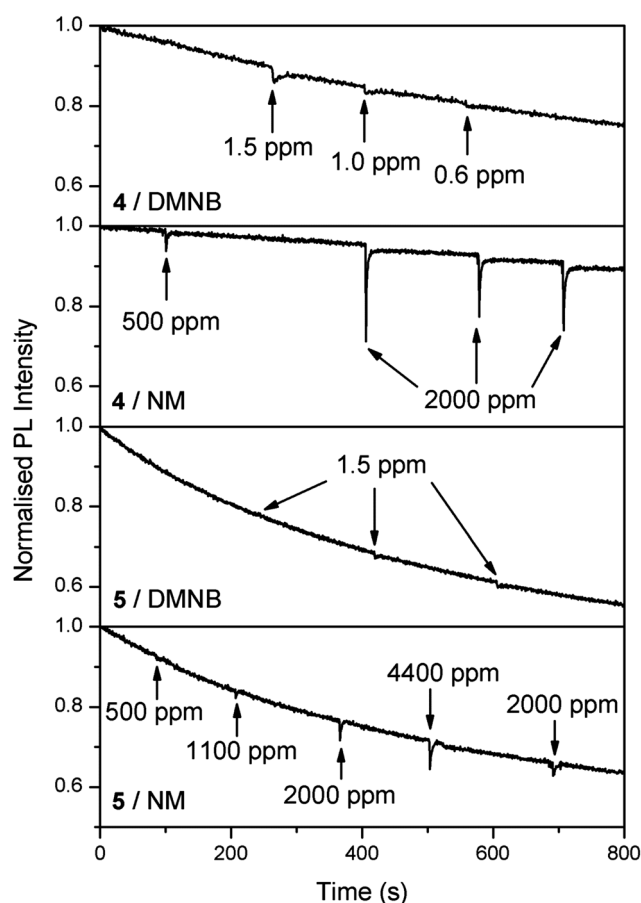


Fig. 6 Thin film quenching of **4** and **5** by DMNB and NM. Traces indicate an 800 s period from a total sampling time of 1800 s. The differences in baseline slope arise from the different times at which sampling was performed during the 1800 s experiments.

intensity in Fig. 6 is due to the relative volatility of the two analytes, with the volumes injected resulting in greater concentrations of NM.

The natural rate of photodegradation of thin films of **5** was greater than that of **4** and made the measurements more difficult to perform. Nevertheless the film measurements were in agreement with the solution-based measurements, with the quenching of the fluorescence of **5** being observed to be weaker than **4** with both analytes. The response of **5** to repeated 1.5 ppm injections of DMNB was very weak (<1% quench) and injections early in the quenching measurements were obscured by the photodegradation of the film. The responses to injections of NM vapour are also weaker than the corresponding interactions with **4** giving an average quenching response of approximately $0.002\% \text{ ppm}^{-1}$ in the concentration range below 4400 ppm. Once again the quenching interaction with NM was reversible with the baseline fluorescence recovering within 10 seconds of exposure. The ability to recover the baseline signal under ambient flow conditions is by no means a ubiquitous quality of films of fluorescent sensing materials with some requiring chemical or thermal treatment to be reactivated for sensing.^{6,12,13} The reversible nature of the quenching interactions of **4** and **5** thin films with the nitroaliphatics is advantageous for a reusable sensing array.

Conclusions

In summary, we have developed two carbazole-containing dendrimers capable of detecting the explosive component analytes DMNB and NM with unparalleled sensitivity in solution. The levels of detection observed are comparable to those of higher electron affinity nitroaromatic analytes with dendrimer systems bearing the same dendrons but different cores.^{17,18} Sensing in solution proceeds predominantly *via* collisional quenching and is facilitated by long excited state lifetimes. In designing more effective fluorescent sensing molecules for high electron affinity targets (whether they be nitroaliphatic or otherwise) one must consider and understand whether static or collisional quenching is the dominant mechanism. Nitroaliphatic detection has been an issue for sensing by oxidative fluorescence quenching and understanding the collisional nature of the quenching interactions plays an important role in improving sensitivity towards DMNB and NM in solution. Traditionally solution-based steady-state Stern–Volmer measurements have been used to screen the sensing potential of a new fluorophore.^{3,4,8–10,13} However, it has been observed that a high Stern–Volmer quenching efficiency whilst useful in a laboratory setting is not necessarily a promising attribute for thin film sensing arrays. For deployment in a portable fluorescence sensor device thin film properties are of the utmost importance. The ability of our system to detect sub-saturation levels of both DMNB and NM reversibly in the solid state is a critical step on the path to developing practical sensing materials.

Experimental details

General methods and synthesis of organic materials

Unless otherwise indicated all chemicals were obtained from commercial suppliers and used as received. Solvents were distilled by rotary evaporation prior to use. Anhydrous tetrahydrofuran for reactions was dried over sodium/benzophenone and distilled immediately prior to use. Thin layer chromatography was performed on Merck aluminium plates coated with silica gel 60 P₂₅₄. Column chromatography was performed with Merck silica gel (0.063–0.200 mm). When solvent mixtures are used the proportions are given by volume.

¹H and ¹³C NMR spectra were recorded on either a Bruker AV400 (400 MHz) or AV500 (500 MHz) spectrometers. Chemical shifts are reported in parts per million (ppm) and are referenced to the residual solvent peak ($\delta_{\text{H}}(\text{CDCl}_3) = 7.26$, $\delta_{\text{C}}(\text{CDCl}_3) = 77.0$). Coupling constants, *J*, are reported in Hertz (Hz) to nearest 0.5 Hz. Peak multiplicities are labelled in the following manner: singlet (s), doublet (d), triplet (t), or multiplet (m). Peak identities are abbreviated as phenyl (Ph) and carbazolyl (Cbz). Peak assignments were made with the aid of ¹³C DEPT, ¹H–¹H COSY, ¹H–¹³C HSQC and ¹H–¹³C HMBC spectra.

Matrix-assisted Laser Desorption Ionisation Time of Flight (MALDI-TOF) mass spectra were recorded on an Applied Biosystems Voyager MALDI-TOF mass spectrometer using dithranol (1,8,9-anthracenetriol) as the matrix. Electrospray ionisation (ESI) mass spectra were recorded on a Bruker HCT 3D Ion Trap with methanol/dichloromethane as solvent.

Elemental analysis was performed by the Microanalytical Service of the School of Chemistry and Molecular Biosciences

at The University of Queensland, Australia. Melting points were measured using a Büchi Melting Point B-545 and are corrected.

UV-Visible absorption spectra were recorded on a Varian Cary 5000 UV-Vis-NIR spectrophotometer in spectrophotometric grade solvent. Absorption λ_{max} values are quoted to the nearest nm and shoulders are denoted by sh. Infrared absorption spectra were measured with a Perkin Elmer Spectrum 100 FT-IR spectrophotometer as neat samples using an ATR interface.

Glass transition temperatures (T_g) were recorded on a Perkin Elmer Diamond DSC Differential Scanning Calorimeter calibrated to an indium standard. Decomposition temperatures (T_{dec}) are quoted for 5% weight decomposition and were recorded using a Perkin Elmer STA 6000 Simultaneous Thermal Analyser under a nitrogen atmosphere.

Cyclic and differential pulse voltammetry was undertaken on a BASi EpsilonEC and values are quoted relative to the ferrocenium/ferrocene couple.³² A silver/silver nitrate in acetonitrile reference electrode was used in combination with platinum or glassy carbon working electrodes and a platinum counter electrode. Acetonitrile for the reference electrode was stored over 3 Å molecular sieves. Solvents for electrochemical measurements were dried and distilled on the day of use. Dichloromethane was dried over calcium hydride and tetrahydrofuran was dried over sodium/benzophenone and distilled before it was dried over and distilled from lithium aluminium hydride.

Gel permeation chromatography was performed on a Polymer Laboratories PL GPC 50 using PLgel 3 μm mixed-E columns (2 \times 300 mm lengths, 7.5 mm diameter) from Polymer Laboratories calibrated against polystyrene narrow standards [$M_p = (162 - 3.8) \times 10^4$] in tetrahydrofuran containing 0.01% toluene as a flow marker. The eluent was degassed with helium and pumped at a rate of 0.5 cm³ min⁻¹ at 39.3 °C. UV absorption at 256 nm was used to detect the eluting species.

Thin films were spin-cast using a Speciality Coating Systems (SCS) G3-8 Spincoater and surface profilometry was performed on a Veeco Dektak 150 to determine the film thicknesses.

Spectroscopy

Photoluminescence (PL) and photoluminescence excitation (PLE) spectra were recorded on a Jobin-Yvon Horiba Fluoromax 4 in spectrophotometric grade solvents. Solution photoluminescence quantum yield (PLQY) measurements were measured relative to quinine sulfate (PLQY = 0.55) in 0.5 M sulfuric acid.²¹ PLQY values were determined from plots of absorbance *versus* integrated PL for the dendrimers relative to that of a quinine sulfate standard (0.02 < *A* < 0.10). The standard errors in the gradients of these plots calculated by least squares regression were propagated using the chain rule to determine the error in PLQY. The error in solution PLQY values was found to be ± 0.01 .

Thin film PLQY measurements were performed using the procedure described by Greenham *et al.*³³ Thin film samples were photoexcited using the 325 nm output of a HeCd laser under nitrogen. Unless otherwise stated the excitation wavelength used for PL measurements was 320 nm.

Solution quenching measurements

An optically dilute (absorbance approximately 0.1 at peak) dendrimer solution was prepared and used as a stock solution. Analyte solutions of known concentration were prepared from the dendrimer stock such that dendrimer concentrations remained constant throughout all measurements. In all experiments the initial dendrimer solution volume was 2.5 cm³ and analyte solutions were added in 0.05 cm³ aliquots.

For steady-state Stern–Volmer measurements the initial absorption and PL spectra of the dendrimer solutions were measured before analyte solutions were added. After each addition of analyte the absorption and PL spectra were again recorded. Addition of the analyte to the solution caused attenuation of the excitation beam and absorption of lower wavelength dendrimer fluorescence due to UV absorption by the analyte. These two effects can be reliably corrected for providing the measurements are done within the Beer–Lambert regime (absorbance ≤ 0.6 at excitation wavelength) and hence the analyte concentrations were selected to ensure that this criterion was fulfilled. All measurements were completed in triplicate with separately prepared analyte solutions. The largest error in the calculation of steady-state Stern–Volmer constants was found to arise from the corrections applied for analyte absorption, specifically in the accurate measurement of wavelengths on the spectrophotometer and fluorometer. We have assumed a tolerance of ± 1 nm in wavelength recognition between the instruments and the error quoted is the deviation in the observed K_{sv} value when varying the excitation wavelength within this range.

Time-resolved Stern–Volmer measurements were performed on a Jobin-Yvon Horiba Fluorolog FL3-11 with a time-correlated single photon counting module. The materials were excited at 372 nm with 1.2 ns pulses and a repetition rate of 1 MHz using the output of a Horiba Scientific NanoLED pulsed diode light source. Fluorescence decays were measured at 400 nm with an instrument response function (IRF) with a FWHM of approximately 1.5 ns. The data was fitted to a single exponential decay following convolution with the IRF. Due to the proximity of the detection and excitation wavelengths scatter of the excitation beam was observed in the decays. The background signal was recorded using spectrophotometric grade toluene as a scatterer, which was subtracted from the observed data prior to fitting. The errors associated with the calculation of the collisional Stern–Volmer constants are generally small due to the lack of corrections needed for analyte absorption. The error quoted is the standard error in the gradient of the time-resolved Stern–Volmer plots calculated by least squares regression.

Thin film quenching measurements

Fused silica substrates (12 mm diameter) were cleaned by rinsing with acetone, 2-propanol (under ultrasonication) and toluene prior to dendrimer deposition. Dendrimer films were spin-cast from 10 mg cm⁻³ solutions in toluene. Dendrimer solutions were pipetted onto the surface of the cleaned substrates until the surface was covered by the solution and the films were immediately spun at 2000 rpm for 2 min (acceleration = 2000 rpm s⁻¹). Under these spinning conditions the film thicknesses were found to be 48 ± 5 nm and 52 ± 6 nm for **4** and **5** respectively. The

substrates were clamped in a custom built sample holder in a Jobin Yvon Horiba Fluorolog Tau fluorometer. The dendrimer film was placed on the opposite side of the substrate to the excitation beam (320 nm, angle of incidence = 60°) and the PL at 400 nm was detected at right angles to the excitation pulse facing the film. A flow of nitrogen (16.7 cm³ s⁻¹) was established into the chamber from an aperture facing the film (angle of incidence = 60°) and held constant throughout the measurement. The flow of nitrogen was controlled by a Bronkhorst EL-FLOW Select mass flow controller calibrated for nitrogen within the flow range 2.5–125 cm³ s⁻¹. The apparatus was purged with nitrogen for 20 min. The PL intensity was then monitored for 30 min during which time analytes were injected. Analytes were introduced by manually injecting a known volume (between 0.2 and 20 cm³) of saturated analyte vapour into the nitrogen carrier stream over 1 s. Cotton wool was placed inside the syringes at the outlet to prevent the injection of particles of analyte into the carrier gas flow. The stoppered syringes were allowed to saturate with analyte vapours at 22 °C overnight prior to injection. The approximate concentration of analyte introduced was estimated from the reported saturated vapour concentrations^{9,31} and the dilution ratio of the analyte in the nitrogen carrier stream.

4-{3,5-Bis[4-(2-ethylhexyloxy)phenyl]phenyl}-2-methylbut-3-yn-2-ol (3). **6**¹⁹ (0.100 g, 0.177 mmol) was dissolved in piperidine (1.4 cm³). Copper(I) iodide (0.002 g, 8.8 μ mol) was added to the solution and the mixture was sparged with nitrogen for 10 min. Tetrakis(triphenylphosphine)palladium(0) (0.010 g, 8.8 μ mol) was added to the mixture, which was then sparged with nitrogen for 10 min. 2-Methylbut-3-yn-2-ol (0.10 cm³, 1.03 mmol) was added and the mixture was stirred at 80 °C for 16 h. The mixture was allowed to cool to room temperature before the volatiles were removed *in vacuo*. The residue was purified by column chromatography over silica using dichloromethane : *n*-hexane (7 : 3) as eluent to yield **3** as an orange oil (0.092 g, 91%). Found C, 82.2; H, 9.4%; C₃₉H₅₂O₃ requires C, 82.4; H, 9.2%. λ_{max} (CH₂Cl₂/nm): 264 (log ϵ /dm³ mol⁻¹ cm⁻¹ = 4.69), 273 sh (4.67). $\bar{\nu}_{max}$ (film, ATR/cm⁻¹): 3349 (br, O–H Stretch), no prominent C≡C stretch was observed. δ_H (500 MHz, CDCl₃): 0.92–0.98 (12H, m, ethylhexyl CH₃), 1.32–1.59 (16H, m, ethylhexyl CH₂), 1.67 (6H, s, HOC(CH₃)₂–), 1.74–1.79 (2H, m, OCH₂CH(C₄H₉)(C₂H₅)), 2.17 (1H, s, HOC(CH₃)₂–), 3.90 (4H, m, OCH₂CH(C₄H₉)(C₂H₅)), 6.99 (4H, $\frac{1}{2}$ AA'BB', surface PhH), 7.54–7.56 (6H, m, branching and surface PhH), 7.66 (1H, dd, J = 2.0 Hz and 2.0 Hz, branching PhH). δ_C (126 MHz, CDCl₃): 11.1, 14.1, 23.0, 23.8, 29.1, 30.5, 31.5, 39.4, 65.6, 70.6, 82.3, 93.6, 114.8, 123.4, 125.2, 128.1 (two overlapping peaks), 132.6, 141.4, 159.2. m/z [ESI⁺]: 551.4 (M – OH⁺), 569.5 (M + H⁺).

3,6-Bis[3,5-bis[4-(2-ethylhexyloxy)phenyl]phenyl]-9-*n*-hexylcarbazole (4). **1**³⁴ (0.076 g, 0.186 mmol) and **2**¹⁹ (0.284 g, 0.464 mmol) were dissolved in toluene (3 cm³). Aqueous potassium carbonate (2 M, 1 cm³) and *tert*-butanol (1 cm³) were added and the mixture was deoxygenated by sparging with nitrogen for 10 min. Tetrakis(triphenylphosphine)palladium(0) (0.011 g, 9.26 μ mol) was added and the mixture was deoxygenated by sparging with nitrogen for 10 min. The mixture was stirred at 100 °C under nitrogen for 4 h before it was allowed to cool to room temperature. The mixture was diluted with toluene (25 cm³) and water (25 cm³) and the

layers were separated. The aqueous layer was extracted with toluene ($2 \times 25 \text{ cm}^3$) and the combined organics were washed with water ($2 \times 25 \text{ cm}^3$) and brine (25 cm^3). The organics were dried over anhydrous magnesium sulfate and the organics decanted. The magnesium sulfate was washed with additional solvent and the decanted organics combined before the volatiles were removed *in vacuo*. The residue was purified by column chromatography over silica using dichloromethane : *n*-hexane (1 : 4–3 : 7) as eluent to yield **4** as an off-white glassy solid (0.119 g, 52%). Found C, 84.6; H, 9.0; N, 1.2%; $\text{C}_{86}\text{H}_{109}\text{NO}_4$ requires C, 84.6; H, 9.0; N, 1.1%. λ_{max} ($\text{CH}_2\text{Cl}_2/\text{nm}$): 259 sh ($\log \epsilon/\text{dm}^3 \text{ mol}^{-1} \text{ cm}^{-1} = 5.19$), 263 (5.20), 281 sh (5.10), 296 sh (4.98), 316 sh (4.54), 336 sh (3.94), 354 sh (3.57). δ_{H} (400 MHz, CDCl_3): 0.92–1.00 (27H, m, hexyl and ethylhexyl CH_3), 1.36–1.57 (38H, m, hexyl and ethylhexyl CH_2), 1.76–1.83 (4H, m, $\text{PhOCH}_2\text{CH}(\text{C}_4\text{H}_9)(\text{C}_2\text{H}_5)$), 1.93–2.00 (2H, m, $\text{NCH}_2\text{CH}_2(\text{C}_4\text{H}_9)$), 3.94 (8H, m, $\text{PhOCH}_2\text{CH}(\text{C}_4\text{H}_9)(\text{C}_2\text{H}_5)$), 4.39 (2H, t, $J = 7.0 \text{ Hz}$, $\text{NCH}_2\text{CH}_2(\text{C}_4\text{H}_9)$), 7.05 and 7.70 (16H, AA'BB', surface PhH), 7.53 (2H, d, $J = 8.5 \text{ Hz}$, CbzH), 7.72 (2H, dd, $J = 1.5 \text{ Hz}$ and 1.5 Hz , branching PhH), 7.85–7.87 (6H, m, overlapping branching PhH and CbzH), 8.50 (2H, d, $J = 1.5 \text{ Hz}$, CbzH). δ_{C} (126 MHz, CDCl_3): 11.3, 14.2, 14.3, 22.7, 23.2, 24.0, 27.2, 29.2, 29.3, 30.7, 31.8, 39.6, 43.5, 70.7, 109.3, 115.0, 119.3, 123.7, 123.8, 124.5, 125.7, 128.5, 132.7, 133.9, 140.7, 142.1, 143.2, 159.3. *m/z* [MALDI-TOF] anal. calcd 1219.8 (100%), 1220.8 (97%), 1221.8 (47%), 1222.8 (15%), 1223.8 (4%). Found 1219.9 (100%), 1220.9 (95%), 1221.9 (55%), 1222.9 (15%). $T_{\text{g}} = 36.8 \text{ }^\circ\text{C}$ (no melting transitions were observed below $200 \text{ }^\circ\text{C}$). $T_{5\% \text{ dec}} = 399.0 \text{ }^\circ\text{C}$. $E_{1/2}(\text{OX}, \text{THF}, \text{CV}) = 0.71 \text{ V}$. GPC, $\bar{M}_{\text{w}} = 1613$, $\bar{M}_{\text{n}} = 1606$, $\bar{M}_{\text{v}} = 1612$.

3,6-Bis({3,5-bis[4-(2-ethylhexyloxy)phenyl]phenyl}ethynyl)-9-*n*-hexylcarbazole (5). 1^{34} (0.050 g, 0.120 mmol), **3** (0.150 g, 0.264 mmol) and tetra-*n*-butylammonium bromide (0.002 g, 5.66 μmol) were dissolved in toluene (3 cm^3). Aqueous sodium hydroxide (20% w/w, 3 cm^3) was added and the mixture was sparged with nitrogen for 10 min. Copper(I) iodide (0.001 g, 5.99 μmol) was added and the mixture was deoxygenated by sparging with nitrogen for 10 min. Tetrakis(triphenylphosphine)palladium(0) (0.007 g, 5.99 μmol) was added and the mixture was deoxygenated by sparging with nitrogen for a further 10 min. The mixture was stirred at $80 \text{ }^\circ\text{C}$ under nitrogen for 4 h and was allowed to cool to room temperature. The mixture was diluted with toluene (25 cm^3) and water (25 cm^3) and the layers were separated. The aqueous layer was extracted with toluene ($2 \times 25 \text{ cm}^3$) and the combined organics were washed with water ($2 \times 25 \text{ cm}^3$) and brine (25 cm^3). The organics were dried over anhydrous magnesium sulfate and the organics were decanted. The magnesium sulfate was washed with additional solvent and the decanted organics combined before the volatiles were removed *in vacuo*. The residue was purified by column chromatography over silica using dichloromethane : *n*-hexane (1 : 4) as eluent to yield **5** as an orange glassy solid (0.071 g, 47%). Found C, 84.9; H, 8.8; N, 1.1%; $\text{C}_{89}\text{H}_{107}\text{NO}_6$ requires C, 85.2; H, 8.7; N, 1.1%. λ_{max} ($\text{CH}_2\text{Cl}_2/\text{nm}$): 269 sh ($\log \epsilon/\text{dm}^3 \text{ mol}^{-1} \text{ cm}^{-1} = 4.91$), 284 (5.01), 314 sh (4.82), 345 (4.67). $\bar{\nu}_{\text{max}}$ (film, ATR/ cm^{-1}): 2207 (w, $\text{C}\equiv\text{C}$ stretch). δ_{H} (500 MHz, CDCl_3): 0.88 (3H, t, $J = 7 \text{ Hz}$, hexyl CH_3), 0.91–0.98 (24H, m, ethylhexyl CH_3), 1.29–1.58 (38H, m, hexyl and ethylhexyl CH_2), 1.75–1.80 (4H, m,

$\text{PhOCH}_2\text{CH}(\text{C}_4\text{H}_9)(\text{C}_2\text{H}_5)$), 1.86–1.92 (2H, m, $\text{NCH}_2\text{CH}_2(\text{C}_4\text{H}_9)$), 3.91 (8H, m, $\text{PhOCH}_2\text{CH}(\text{C}_4\text{H}_9)(\text{C}_2\text{H}_5)$), 4.31 (2H, t, $J = 7.0 \text{ Hz}$, $\text{NCH}_2\text{CH}_2(\text{C}_4\text{H}_9)$), 7.01 and 7.61 (16H, AA'BB', surface PhH), 7.40 (2H, d, $J = 8.5 \text{ Hz}$, CbzH), 7.69–7.72 (8H, m, branching PhH and CbzH), 8.34 (2H, d, $J = 1.5 \text{ Hz}$, CbzH). δ_{C} (126 MHz, CDCl_3): 11.1, 14.0, 14.1, 22.5, 23.1, 23.9, 26.9, 28.9, 29.1, 30.5, 31.5, 39.4, 43.4, 70.6, 88.1, 90.5, 109.0, 113.9, 114.9, 122.5, 124.2, 124.5, 124.9, 128.0, 128.2, 129.8, 132.8, 140.5, 141.5, 159.3. *m/z* [MALDI-TOF] anal. calcd 1267.8 (97%), 1268.8 (100%), 1269.8 (51%), 1270.8 (17%), 1271.8 (5%). Found 1268.0 (87%), 1269.0 (100%), 1269.9 (56%), 1270.9 (15%). $T_{\text{g}} = 25.1 \text{ }^\circ\text{C}$. $T_{5\% \text{ dec}} = 399.8 \text{ }^\circ\text{C}$. $E_{1/2}(\text{OX}, \text{DCM}, \text{DPV}) = 0.75 \text{ V}$. GPC, $\bar{M}_{\text{w}} = 1863$, $\bar{M}_{\text{n}} = 1856$, $\bar{M}_{\text{v}} = 1862$.

9-*n*-Hexylcarbazole was prepared by a literature procedure³⁵ for optical studies.

Acknowledgements

The Authors acknowledge funding from the Australian Research Council (DP0986838) and The University of Queensland (Strategic Initiative – Centre for Organic Photonics & Electronics). AJC is supported by an Endeavour International Postgraduate Research Scholarship and a University of Queensland Research Scholarship. PLB is supported by an Australian Research Council Federation Fellowship (Project no. FF0668728). PM is supported by a University of Queensland Vice Chancellor's Senior Research Fellowship.

References

- 1 A. W. Czarnik, *Nature*, 1998, **394**, 417.
- 2 J.-S. Yang and T. M. Swager, *J. Am. Chem. Soc.*, 1998, **120**, 11864.
- 3 S. J. Toal and W. C. Trogler, *J. Mater. Chem.*, 2006, **16**, 2871.
- 4 M. Guo, O. Varnavski, A. Narayanan, O. Mongin, J.-P. Majoral, M. Blanchard-Desce and T. Goodson III, *J. Phys. Chem. A*, 2009, **113**, 4763.
- 5 H. Cavaye, A. R. G. Smith, M. James, A. Nelson, P. L. Burn, I. R. Gentle, S.-C. Lo and P. Meredith, *Langmuir*, 2009, **25**, 12800.
- 6 G. Tang, S. S. Y. Chen, P. E. Shaw, K. Hegeudus, X. Wang, P. L. Burn and P. Meredith, *Polym. Chem.*, 2011, **2**, 2360.
- 7 J. C. Sanchez, S. J. Toal, Z. Wang, R. E. Dugan and W. C. Trogler, *J. Forensic Sci.*, 2007, **52**, 1308.
- 8 J. C. Sanchez, A. G. DiPasquale, A. L. Rheingold and W. C. Trogler, *Chem. Mater.*, 2007, **19**, 6459.
- 9 S. W. Thomas III, J. P. Amara, R. E. Bjork and T. M. Swager, *Chem. Commun.*, 2005, 4572.
- 10 M. E. Germain and M. J. Knapp, *Chem. Soc. Rev.*, 2009, **38**, 2543.
- 11 K. J. Balkus Jr, T. J. Pisklak, G. Hundt, J. Sibert and Y. Zhang, *Microporous Mesoporous Mater.*, 2008, **112**, 1.
- 12 A. Lan, K. Li, H. Wu, D. H. Olson, T. J. Emge, W. Ki, M. Hong and J. Li, *Angew. Chem., Int. Ed.*, 2009, **48**, 2334.
- 13 T. Naddo, X. Yang, J. S. Moore and L. Zang, *Sens. Actuators, B*, 2008, **134**, 287.
- 14 D. Jones, R. Augsten and K. Feng, *J. Therm. Anal. Calorim.*, 1995, **44**, 533.
- 15 S. B. Markofsky, *Ullman's Encyclopedia of Industrial Chemistry*, Wiley-VCH Verlag GmbH & Co, 2000.
- 16 M. E. Germain, T. R. Vargo, P. G. Khalifah and M. J. Knapp, *Inorg. Chem.*, 2007, **46**, 4422.
- 17 D. A. Olley, E. J. Wren, G. Vamvounis, M. J. Fernee, X. Wang, P. L. Burn, P. Meredith and P. E. Shaw, *Chem. Mater.*, 2010, **23**, 789.
- 18 H. Cavaye, P. E. Shaw, X. Wang, P. L. Burn, S.-C. Lo and P. Meredith, *Macromolecules*, 2010, **43**, 10253.
- 19 S.-C. Lo, E. B. Namdas, P. L. Burn and I. D. W. Samuel, *Macromolecules*, 2003, **36**, 9721.

- 20 P. L. Burn, R. Beavington, M. J. Frampton, J. N. G. Pillow, M. Halim, J. M. Lupton and I. D. W. Samuel, *Mater. Sci. Eng., B*, 2001, **85**, 190.
- 21 J. N. Demas and G. A. Crosby, *J. Phys. Chem.*, 1971, **75**, 991.
- 22 S. Dong, Z. Li and J. Qin, *J. Phys. Chem. B*, 2008, **113**, 434.
- 23 J. R. Lakowicz, *Principles of Fluorescence Spectroscopy*, Springer, New York, 3rd edn, 2006.
- 24 W. J. Aixill, P. B. Mills, R. G. Compton, F. Prieto and M. Rueda, *J. Phys. Chem. B*, 1998, **102**, 9187.
- 25 S. F. Alvarado, P. F. Seidler, D. G. Lidzey and D. D. C. Bradley, *Phys. Rev. Lett.*, 1998, **81**, 1082.
- 26 H. Cavaye, H. Barcena, P. E. Shaw, P. L. Burn, S.-C. Lo and P. Meredith, Organic semiconductors in sensors and bioelectronics II, *Proc. SPIE*, 2009, **7418**, 741803.
- 27 D. Zhao and T. M. Swager, *Macromolecules*, 2005, **38**, 9377.
- 28 S. W. Thomas III, G. D. Joly and T. M. Swager, *Chem. Rev.*, 2007, **107**, 1339.
- 29 P. Atkins and J. de Paula, *Atkins' Physical Chemistry*, Oxford University Press, Oxford, 8th edn, 2006.
- 30 G. E. Johnson, *J. Phys. Chem.*, 1980, **84**, 2940.
- 31 W. M. Jones and W. F. Giauque, *J. Am. Chem. Soc.*, 1947, **69**, 983.
- 32 B. W. D'Andrade, S. Datta, S. R. Forrest, P. Djurovich, E. Polikarpov and M. E. Thompson, *Org. Electron.*, 2005, **6**, 11.
- 33 N. C. Greenham, I. D. W. Samuel, G. R. Hayes, R. T. Phillips, Y. A. R. R. Kessener, S. C. Moratti, A. B. Holmes and R. H. Friend, *Chem. Phys. Lett.*, 1995, **241**, 89–96.
- 34 C. Beginn, J. V. Gražulevičius, P. Strohmriegl, J. Simmerer and D. Haarer, *Macromol. Chem. Phys.*, 1994, **195**, 2353.
- 35 H. Wang, G. Chen, X. Xu, H. Chen and S. Ji, *Dyes Pigm.*, 2010, **86**, 238.